Check for updates

Aqueous titanium redox flow batteries—State-of-the-art and future potential

Sheikh Imran Uddin Ahmed[1†], Mohamed Shahid[1,2†] and
Shrihari Sankarasubramanian[1,3,4]*

[1]Department of Biomedical Engineering and Chemical Engineering, University of Texas at San Antonio,
San Antonio, TX, United States, [2]Department of Chemical Engineering, University of Petroleum and
Energy Studies, Dehradun, India, [3]NASA MIRO Center for Advanced Measurements in Extreme
Environments (CAMEE), University of Texas at San Antonio, San Antonio, TX, United States, [4]Texas
Sustainability Research Institute (TSERI), University of Texas at San Antonio, San Antonio, TX,
United States

Market-driven deployment of inexpensive (but intermittent) renewable energy
sources, such as wind and solar, in the electric power grid necessitates grid-
stabilization through energy storage systems Redox flow batteries (RFBs), with
their rated power and energy decoupled (resulting in a sub-linear scaling of cost),
are an inexpensive solution for the efficient electrochemical storage of large
amounts of electrical energy. Titanium-based RFBs, first developed by NASA in
the 1970s, are an interesting albeit less examined chemistry and are the focus of
the present review. Ti, constituting 0.6% of the Earth's crust and an ingredient in
inexpensive white paints, is amongst the few elements (V and Mn being some
others) which exhibit multiple soluble oxidation states in aqueous electrolytes.
Further, the very high (approaching 10 M) solubility of Ti in low pH solutions
suggests the possibility of developing exceptionally high energy density aqueous
Redox Flow Batteries systems. With these advantages in mind, we present the
state-of the-art in Ti-RFBs with a focus on Ti/Mn, Ti/Fe and Ti/Ce couples and
systems that use Ti as an additive (such as Ti/V/Mn). The inherent advantages of
inexpensive Ti actives and relatively high energy density is contrasted with
potential side-reactions resulting in reduced energy efficiency. Technological
pathways are presented with a view to overcoming critical bottlenecks and a
vision is presented for the future development of Ti-RFBs.

KEYWORDS

energy storage, redox flow batteries, titanium, kinetics, solvation, energy storage
(batteries)

1 Introduction

The rapid, market-driven deployment of economical but intermittent renewable
energy sources such as solar and wind necessitates the integration of reliable energy
storage solutions with the electric grid to ensure grid stability and reliability. Amongst
various energy storage technologies redox flow batteries (RFBs) are an economical
solution at scale due to their characteristic decoupling of energy and power that

ensures sublinear scaling of cost (Chen et al., 2009; Zhao et al., 2015). A plethora of possible RFBs have been investigated and proposed in the literature, such as, Fe-X (X = Cr, Mn, Fe, Zn) (Fedkiw and Watts, 1984; Skyllas-Kazacos et al., 2011; Gong et al., 2016; Selverston et al., 2017; Archana et al., 2020; Zhen et al., 2020), V-X (X = Mn, Ce, Br, V) (Chen et al., 2009; Prifti et al., 2012; Cunha et al., 2015; Zhao et al., 2015; Sankarasubramanian et al., 2019; Reynard et al., 2020; Raja et al., 2021; Wang et al., 2021) and Zn-X (X = Ce, Br, Mn, V) (Chen et al., 2009; Leung et al., 2011; Dewage et al., 2015; Zhao et al., 2015; Jiang et al., 2018; Ulaganathan et al., 2019; Naresh et al., 2021) RFBs. Critically, the translation of these RFBs to the market hinges on numerous factors, namely - 1) cell potential, 2) energy density (a function of salt solubility in the electrolyte), 3) chemical and electrochemical stability of the cell components, and finally (and possibly most importantly) 4) availability of the redox active species at low marginal cost and at scale. The energy storage cost of RFBs hinges on the cost of the electrolyte actives and their degradation and loss during operation. The loss of electrolyte due to crossover results in poor coulombic efficiency at the system level and hinders economical operation. The crossover of electrolyte species is largely determined by the nature of the separator employed. Three classes of separators are typically encountered in RFBs i.e., cation exchange membrane (CEM), anion exchange membrane (AEM), and porous membrane (PM) (Varcoe et al., 2014; Barry et al., 2021). The two classes of ion exchange membranes operate on the principle of charge-based repulsion and hence exclusion of redox active species. Selectivity is conferred by the nature of the charged species attached to the separator backbone and density of these species. Porous separators, on the other hand, rely on size-based exclusion of redox active species. Here, ionic species and chemical species in solution (irrespective of charge) are prevented from crossing over on the basis of their size relative to the pores across the separator. CEMs (typically Nafion®) are relatively expensive and exhibit high ionic conductivity. Given that most RFBs utilize cationic redox species, the use of CEMs in these systems results in cation cross-over and hence a drastic reduction in capacity over time (Gubler, 2019). This makes CEMs suitable only for systems employing catholytes and anolytes consisting of different oxidation states of the same chemical species (e.g., V^{2+}/V^{3+} and V^{4+}/V^{5+} in all-V RFBs). AEMs, on the other hand, mitigate cation crossover but typically exhibit lower ionic conductivity and chemical stability compared to CEMs (Barry et al., 2021). PMs allow the cross-over of the ions that have smaller diameter than the pore size of the separator irrespective of the nature of the charge they carry and hence show poor ion selectivity (Lu et al., 2017). All separators may require mechanical rebalancing to adjust the osmotic pressure (Bhattarai et al., 2019) and chemical rebalancing to maintain electrolyte purity (Wu et al., 1983; Fedkiw and Watts, 1984).
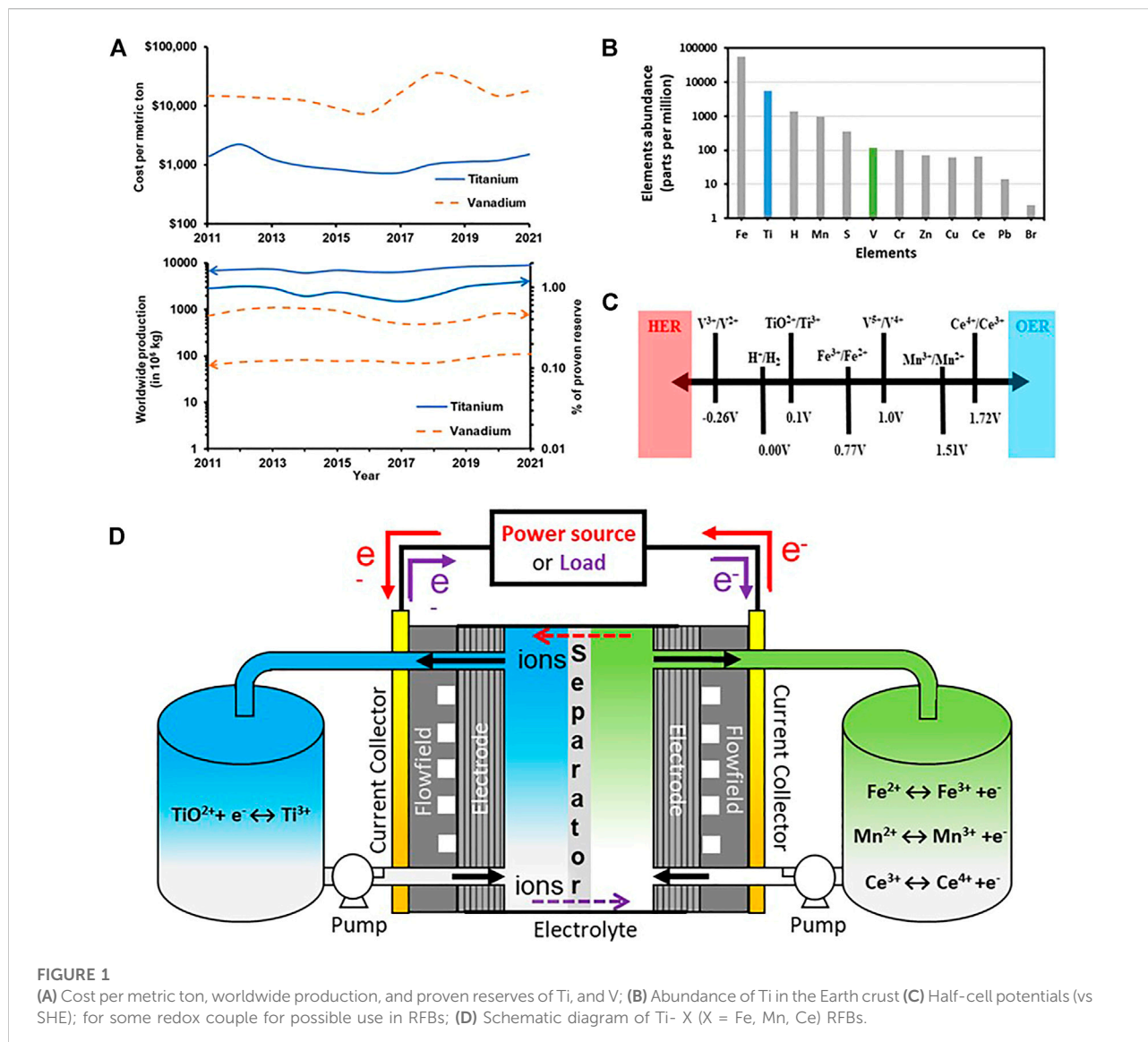
All-V RFBs are the farthest along the commercialization route and have been reported to operate at typical power densities of 100 mW cm^{-2} with cycle life of 10–15 years with 1000 cycle per year (Holland-Cunz et al., 2018). A recent study has reported small, lab-scale (4cm^2 electrode area, 20 ml catholyte and anolyte) all-V RFB operating for ~20,000 cycles at 600 mA cm^{-2} (>8 months) (Jiang et al., 2020). Despite concerns stemming from component degradation while operating at such current densities, the demonstration of similar cycle life (even at lower current density) at a practical, pilot scale would be a major advancement in commercializing all-V RFBs. Although the V-X family of RFBs are quite successful in terms of providing high power densities with stability, the availability of V in the earth's crust and its susceptibility to degradation during cycling is a limiting factor for successful industrialization. On the other hand, the Ti-X (X = Fe, Mn, Ce) family of RFBs offer several advantages over the V-X systems as -

1) Ti is *ca* 50x as abundant as V in the Earth's crust and is produced at *ca* 100x the rate of V (Figures 1A,B).
2) The market price of Ti is 1/10th that of V in the US (Figures 1A,B).
3) The half-cell potential of Ti^{4+}/Ti^{3+} redox couple is 0.1 V (vs SHE) as compared to -0.26 V (vs SHE) for V^{3+}/V^{2+} which makes Ti^{4+}/Ti^{3+} redox couple less prone to hydrogen evolution side reactions (Figure 1C).
4) The maximum possible storage capacity of Ti-Ce RFBs would be 9.9 TWh as compared to 6.95 TWh for all-V RFBs considering all exploitable worldwide reserves of V, Ti, and Ce.
5) The Ti-X (X = Fe, Mn, Ce) RFBs also meets the DOE cost target of <100 \$/kWh (Dong et al., 2015; Kaku et al., 2016; Funding opportunity announcement advanced research projects agency, 2016; Kaku et al., 2019; Sankarasubramanian et al., 2021).

Given these advantages, in this work we critically review the developmental state of Ti-X RFBs and chart a course for their future development.

2 The Ti-X (X = Fe, Mn, Ce) family of RFBs

A schematic representation of Ti-X RFBs is shown in Figure 1D. The anolyte is the Ti salt dissolved in an acid and the catholytes are either Fe or Mn or Ce dissolved in their appropriate acidic counterparts. As discussed in literature, the oxidation states of Ti vary from +2 to +4 and the Ti ions exist stable in the salts as Ti^{3+} (+3 oxidation state), and TiO^{2+} (+4 oxidation state) but not as Ti^{2+}. Their stability is confined to a very narrow region i.e., ~1 pH and lesser, as seen in the Pourbaix diagram (Pourbaix, 1966). TiOSO$_4$ (titanium

FIGURE 1
(A) Cost per metric ton, worldwide production, and proven reserves of Ti, and V; **(B)** Abundance of Ti in the Earth crust **(C)** Half-cell potentials (vs SHE); for some redox couple for possible use in RFBs; **(D)** Schematic diagram of Ti- X (X = Fe, Mn, Ce) RFBs.

oxysulfate) and TiCl$_3$ (titanium chloride) with Ti in +4 and +3 oxidation state are the most widely used salts for Ti-X RFBs with supporting electrolytes including H$_2$SO$_4$, HCl, HNO$_3$ and H$_3$PO$_4$. Thus, the solvation and coordination of Ti species in the strong acidic electrolytes influences the reversibility and stability of the Ti^{4+}/Ti^{3+} redox couple and impacts the energy density of the Ti-X RFBs. The following section summarizes Ti solution chemistry in the context of RFBs.
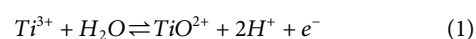
2.1 Ti^{4+} complexes in acids

Extensive literature report (Lingane and Kennedy, 1956; Miyanaga et al., 1990; Kavan et al., 1993; Cservenyák et al., 1996; Sole, 1999; Bahdad, 2020; Tsurumura et al., 2020; Choe et al., 2021) the solvation behavior of Ti^{4+}/Ti^{3+} redox couple with different ligands in various acids solutions like H$_2$SO$_4$, HCl, HNO$_3$ and H$_3$PO$_4$. The redox stability of Ti^{4+}/Ti^{3+} is influenced by the formation of different reaction/intermediate complexes that appear in various acids as discussed below. Critically, we are considering only strong mineral acids in our discussion given that the Ti^{4+}/Ti^{3+} redox couple is stable only in low pH (< *ca* pH 1.5) conditions.

2.1.1 The H$_2$SO$_4$ system

In case of H$_2$SO$_4$ solution comprising dissolved TiOSO$_4$ salt, hereafter called the Ti-O-SO$_4$ system, the half-cell reaction is represented by the following equation,

$$Ti^{3+} + H_2O \rightleftharpoons TiO^{2+} + 2H^+ + e^- \qquad (1)$$

FIGURE 2
Schematic representation of various Ti^{4+} complexes under weakly and strongly acidic conditions.
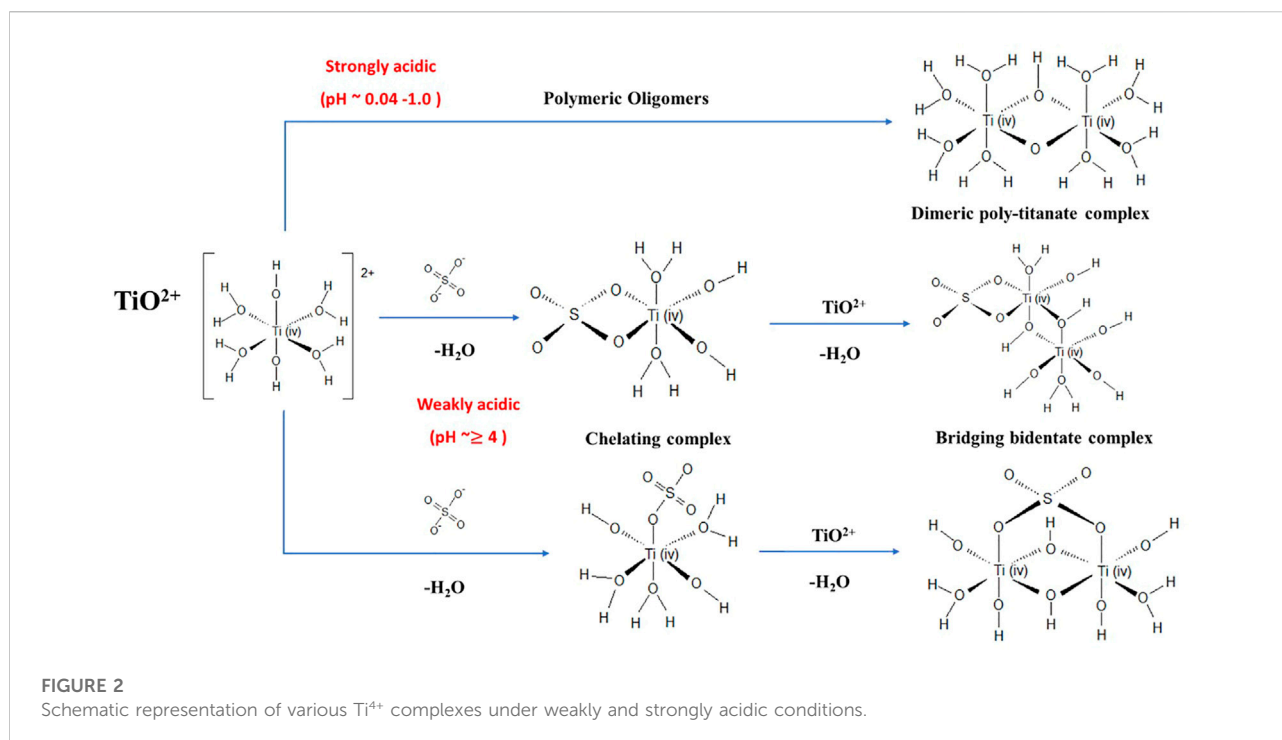
The Ti^{3+} and Ti^{4+} (i.e., as TiO^{2+}) species of the redox couple co-exist in the concentrated Ti-SO$_4$ system. Ti^{4+} is the most stable oxidation state of Ti. The high charge density (ratio of charge to ionic radius) of Ti^{4+} prevents it from forming simply hydrated [Ti(H$_2$O)$_6$]$^{4+}$ (Miyanaga et al., 1990). Ti^{4+} appears as [Ti(OH)$_2$(H$_2$O)$_4$]$^{2+}$ in 1 M H$_2$SO$_4$ aqueous solutions (Bahdad, 2020) and in solutions where 0.04 < pH < 1 (Beukenkamp and Herrington, 1960; Kotsyubynsky et al., 2017), represented in short as TiO^{2+}. These TiO^{2+} complexes tend to form oligomers (Figure 2A) when the oxo-oxygen of the titanyl ion is readily protonatable through hydrolysis reactions (Shepherd, 2013). The formation of oligomers is predominant when the concentration of TiO^{2+} is between 0.1–0.5 M, the H$^+$ concentration between 1.0–2.5 M, and the temperature between 236–323 K (Comba and Merbach, 1987). In the presence of H$^+$, SO$_4^{2-}$ and HSO$_4^-$–ions (H$_2$SO$_4$ dissociation products in an aqueous solution (Choe et al., 2021)), Ti^{4+} forms complexes containing SO$_4^{2-}$ or HSO$_4^-$ ligands exhibiting the possible structures shown in Figure 2B. The competing coordination of Ti^{4+} to SO$_4^{2-}$ or HSO$_4^-$ depends on the strength of SO$_4^{2-}$ concentration in the electrolyte [for e.g., 3 M H$_2$SO$_4$ concentration results in the dominance of Ti^{4+} to SO$_4^{2-}$ coordination (Bahdad, 2020)]. The coordination of HSO$_4^-$ with Ti^{4+} proceeds through a deprotonation pathway wherein H$^+$ is accepted by a proton acceptor such as H$_2$O to form H$_3$O$^+$ or Ti=O$^+$ to form Ti-OH SO$_4^{2-}$ and a Ti^{4+}-SO$_4^{2-}$ complex results. At higher SO$_4^{2-}$ concentrations (and higher pH values), Ti^{4+} is predicted to exist as either mononuclear complexes (chelating complexes) or 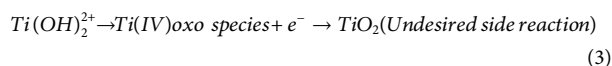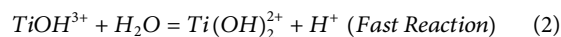multinuclear complexes (bridging bidentate complexes) (Kotsyubynsky et al., 2017). Mononuclear complexes are formed by the coordination of Ti^{4+} ion with SO$_4^{2-}$ leading to formation of [Ti(OH)$_2$SO$_4$(H$_2$O)$_3$]^0, [Ti(OH)$_2$(SO$_4$)$_2$(H$_2$O)$_2$]$^{2-}$ and [Ti=O(OH)$_2$(H$_2$O)$_3$]^0. The multinuclear complexes are formed either due to polymerized Ti^{4+} complexes formed *via* oxygen atoms leading to -Ti-O-Ti-O-zigzag structures (Tsurumura et al., 2018) or *via* formation of [Ti$_2$O$_2$(H$_2$O)$_5$(OH)$_2$SO$_4$] (Choe et al., 2021). These Ti^{4+} complexes are either electrically neutral or anionic in the Ti-O-SO$_4$ system under high pH conditions. Ti^{4+} tends to form multinuclear complexes (nanoscale aggregates) in solutions of high SO$_4^{2-}$ and Ti^{4+} concentrations which eventually results in the nucleation and precipitation to TiO$_2$. Thus, high pH conditions (typically with high SO$_4^{2-}$ concentrations and low H$^+$ concentration) are to be avoided when designing electrolytes for Ti RFBs.

Upon electrochemical reduction of Ti^{4+} to Ti^{3+}, there occurs substantial change in the structures of Ti-ion complexes and nanoscale Ti^{4+} aggregates are gradually disrupted to yield mononuclear Ti^{3+} complexes (Tsurumura et al., 2020). The Ti^{3+} ion is stable at very low pH (< *ca* 1.5) as seen through Pourbaix diagram. In dilute (higher pH) aqueous solutions, Ti^{3+} usually exists in the form of [Ti(H$_2$O)$_6$]$^{3+}$. Literature also report using EXAFS (Extended X-ray Absorption Fine Structure) analysis, that Ti-Ti bond does not exist in Ti^{3+} solution, and the possibility for Ti-O bond exists in Ti^{3+} solution (Miyanaga et al., 1990) with Ti^{3+} ions existing in various other forms in aqueous solutions as Ti(OH)$^{2+}$, TiO$^+$, Ti(OH)$_2^+$, and other complexes (Sole, 1999). However, with

H_2SO_4 solution, Ti^{3+} react with SO_4^{2-} ion to form Ti^{3+}-SO_4^{2-} complexes (Cservenyák et al., 1996).

2.1.2 The HCl system

In case of HCl solutions containing $TiCl_3$ salt, both the H^+ and Cl^- ions play a significant role in the reversibility of Ti^{4+}/Ti^{3+} redox couple. Ti^{3+} exist as a $TiOH^{3+}$ complex in acidified solutions (pH 2–2.5) and, due to hydrolysis of Ti^{3+}, $Ti(OH)_2^{2+}$ is formed with proton liberation as shown below (Kavan et al., 1993; Lokhande et al., 2004),

$$TiOH^{3+} + H_2O = Ti(OH)_2^{2+} + H^+ \ (Fast \ Reaction) \quad (2)$$

$$Ti(OH)_2^{2+} \rightarrow Ti(IV)oxo\ species + e^- \rightarrow TiO_2 (Undesired\ side\ reaction) \quad (3)$$

Unfortunately, $Ti(OH)_2^{2+}$ leads to the formation of TiO_2 by precipitation as shown above, through an intermediate Ti(iv)oxo species which limits the reversibility of the redox couple. The Ti(iv)oxo species consist of partly dehydrated polymeric Ti(IV) hydroxide (Kavan et al., 1993), which get converted to TiO_2 (Lokhande et al., 2005). The Ti^{4+} ions in HCl exist in the form of $TiOCl^+$, an oxy-chloro ion which reduces to a Ti^{3+} chloro complex, $TiCl_4^-$ as shown below,

$$TiOCl^+ + e^- + 2H^+ + 3Cl^- = TiCl^{4-} + H_2O \quad (4)$$
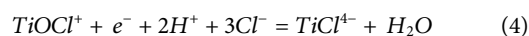
The Ti^{3+}/Ti^{4+} redox couple was found to be reversible only in >1 M HCl solution. The irreversibility observed in <1 M HCl solutions indicates the necessity of Cl^- ion for the reversibility of Ti^{4+} and Ti^{3+} as shown in Eq. 4 (Lingane and Kennedy, 1956). In the presence of HCl and H_2O, Ti^{4+} ions form unstable $[Ti(OH)_2(H_2O)_4]Cl_2$ which eventually results in the formation of TiO_2. In the context of RFBs requiring high reversibility of the Ti^{4+}/Ti^{3+} redox couple, addition of (unfortunately unstable) organic compounds with oxygen-containing functional groups, such as acetylacetone, can partially suppress the hydrolysis reaction owing to the affinity between TiO^{2+} and oxygen-containing functional groups (Wang et al., 1984). HCl concentrations up to 6 M have been found to mitigate the precipitation of TiO_2 (Qiao et al., 2022). However, it enhances H^+ concentration in the electrolyte and accelerates another undesired side reaction, namely the hydrogen evolution reaction (HER), thereby decreasing the RFB efficiency. The choice of the catholyte to be paired with the Ti anolyte can also preclude the use of HCl supporting electrolytes due to the occurrence of the chlorine evolution reaction (+1.36V vs. SHE).

2.1.3 The HNO₃ system

In case of HNO_3 solutions containing $TiOSO_4$, the salt dissolves as small clusters as observed through Small-angle X-ray scattering (SAXS) experiments (Molina et al., 2017). The analysis of $TiOSO_4$ dissolved in 1 M HNO_3 solution, suggests that the clusters contain a dense 1.2 nm diameter core (dominated by Ti–oxo) with a dynamic shell of water, sulfate, and nitrate which also results in precipitation for any dilution below 0.25 M $TiOSO_4$ (Molina et al., 2017). No complexation of Ti^{4+} was observed in dilute HNO_3 solutions (0.73–2.2 mM.L^{-1}) with 0.05 mM.L^{-1} ortho-titanic acid (TiH_4O_4) due to their weak tendency to form nitrato complexes with most metal ions (Morris et al., 1978). This is markedly different from the formation of divalent mononuclear species like $[Ti(OH)_2]^{2+}$ in H_2SO_4 solutions (Mangold et al., 2021). But, however HNO_3 is not actively used as supporting electrolyte due to the reduction of NO^{3-} leading to degraded performance during cycling in RFBs (Xie et al., 2011a).
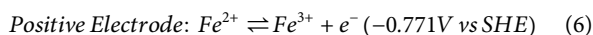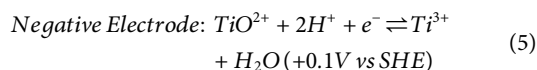
2.1.4 The H₃PO₄ system

Studies with H_3PO_4 solutions containing Ti salts are very scarce in the literature (Lingane and Kennedy, 1956; Oldenburg et al., 2018; Mangold et al., 2021) as the solubility and stability of Ti^{4+} ions in these systems is a practical limitation (Lingane and Kennedy, 1956). The reversibility of Ti^{4+}/Ti^{3+} redox couple and their stability was studied under different concentrations (1–10 M) of H_3PO_4 with 10 mM and lower concentrations of Ti^{4+} [as the $Ti(OH)_4$ salt]. It was found that a 10 mM solution of Ti^{4+} ions in 1M H_3PO_4 was unstable and precipitated after 24 h but stabilized in 4M H_3PO_4 without any phase separation. But upon increasing the Ti^{4+} ion concentrations to >10 mM, the electrolyte was again unstable in 4M H_3PO_4 leading to precipitation. Interestingly, the reversibility of Ti^{4+}/Ti^{3+} redox couple is more pronounced at 1M H_3PO_4 as compared to 4M H_3PO_4 (Shepherd, 2013). In this electrolyte system, Ti^{4+} is present as mononuclear ($\mu = 1$) or polynuclear ($\mu > 1$) free cation(s), $[(TiO)_\mu]^{2\mu+}$ in diluted H_3PO_4 solutions (<0.1 mol.L^{-1}). Ti^{4+} ions progressively form $[(TiO)_\mu(H_{3-m}PO_4)_\delta]^{2\mu-\delta m}$ complexes as the concentration of H_3PO_4 is increased to >1 mol.L^{-1} and $[(TiO)_\mu(H_{3-m}PO_4)_\delta(H_{3-n}PO_4)_\beta]^{2\mu-\delta m-\beta n}$ complexes at >6 mol.L^{-1} H_3PO_4 (Mangold et al., 2021). The poor solubility and reversibility of Ti solutions in H_3PO_4 precludes their use in RFBs.

2.2 Performance of Ti RFBs

Given the discussion above, reports on the Ti-X family of RFBs consist predominantly of systems using H_2SO_4 as the supporting electrolyte due to the stability and reversibility of the Ti^{4+}/Ti^{3+} redox couple at relatively high Ti concentrations (~0.5–1.5 M). This configuration also avoids any side reactions (H_2-, Cl_2-, and NO_2- evolution) thereby increasing the overall energy efficiency of the RFBs.

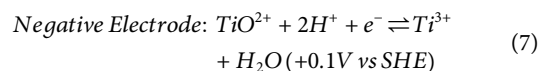*Ti - Fe RFB*: Fe based RFBs (coupled with Ti or Cr) have been widely investigated by NASA in the early 1970s due to the low cost and abundant supply of Fe. These RFBs can achieve a theoretical energy density of nine Wh. L^{-1} (at 0.67V open circuit potential (OCP)). Cr-Fe RFBs was initially assessed for space applications and scale-up studies were conducted, but the system was not commercially developed due to several drawbacks

like, low energy density of the mixed electrolyte (containing both Fe and Cr in the anolyte and catholyte), membrane fouling, the slow Cr redox kinetics requiring expensive noble metal catalysts and parasitic HER on the Cr side (Skyllas-Kazacos et al., 2011). The Ti-Fe RFBs was studied by Thaller in aqueous HCl solution (Thaller and inventor, 1976). In this system, during the charge cycle, Ti^{4+} (i.e., TiO^{2+}) reduced to Ti^{3+} on the negative side and Fe^{2+} is oxidized to Fe^{3+} in positive side. The half-cell charge reactions of the Ti-Fe RFB are,

$$Negative\ Electrode: TiO^{2+} + 2H^+ + e^- \rightleftharpoons Ti^{3+}$$
$$+ H_2O\ (+0.1V\ vs\ SHE) \tag{5}$$

$$Positive\ Electrode: Fe^{2+} \rightleftharpoons Fe^{3+} + e^-\ (-0.771V\ vs\ SHE) \tag{6}$$

Initially, $TiCl_3$ and $FeCl_3$ were the salts used at the anolyte and catholyte respectively in the HCl supported electrolytes. This system suffered from the formation of TiO_2 particles as an undesired side reaction, decreasing the overall coulombic efficiency. The maximum current density of these initial Ti-Fe RFBs with HCl supporting electrolyte was 8.16–14 $mAcm^{-2}$ with a nominal cell voltage around 0.67V (Savinell et al., 1979). Recent improvements in Ti-Fe RFBs have consisted of using H_2SO_4 as supporting electrolyte instead of HCl and using $TiOSO_4$ and $FeSO_4$ salts in the anolyte and catholyte respectively. In the presence of H_2SO_4, the interaction between H_2O and Ti^{4+} ions are diminished, thereby inhibiting the formation of $Ti(OH)_2^{2+}$ and improving the stability of the electrolyte. Such as second generation Ti-Fe RFB with bismuth (Bi) catalyst at the positive electrode and a carbon felt at the negative electrode exhibited a diffusion coefficient of $19.18\times10^{-8}cm^2\ s^{-1}$ for Fe^{3+}/Fe^{2+} and $0.36\times10^{-8}cm^2\ s^{-1}$ for Ti^{4+}/Ti^{3+} (Qiao et al., 2022) with a rate constant of $3.828\times10^{-4}cm\ s^{-1}$ for Fe^{3+}/Fe^{2+} and $0.203\times10^{-4}cms^{-1}$ for Ti^{4+}/Ti^{3+} respectively (Qiao et al., 2022). It suggests that both the diffusion coefficient and rate constant for Fe^{3+}/Fe^{2+} is higher than Ti^{4+}/Ti^{3+} with the reactions of Ti redox couple being rate limited. The Ti-Fe RFBs in 3M H_2SO_4 were cycled at current densities as high as 120 $mAcm^{-2}$ with the highest energy efficiency of 85.6% (at 40 $mAcm^{-2}$). This system showed 80% discharge capacity after 1000 cycles (30 min per cycle) with a low-capacity decay of 0.193 Ah. $cycle^{-1}$ (Qiao et al., 2022). CEMs like Nafion® 212, sulfonated poly (ether ketone) (SPEEK) have been used in Ti-Fe RFB. Non-fluorinated SPEEK is predominantly used as it reduces the cost for energy production from \$165.79/kWh (Nafion® 212) to \$88.22/kWh (SPEEK) (Qiao et al., 2022).

Ti-Mn RFB: Ti-Mn RFBs was first developed by Dong et al, (2012) where a relatively high OCP of 1.41 V was obtained (as compared to 0.67 V for Ti-Fe RFBs) resulting in superior power density (Dong et al., 2015; Kaku et al., 2016). These RFBs can achieve a theoretical energy density of 18.9 Wh. L^{-1}. The half-cell charge redox reactions of Ti-Mn RFB are represented by the following equations.

$$Negative\ Electrode: TiO^{2+} + 2H^+ + e^- \rightleftharpoons Ti^{3+}$$
$$+ H_2O\ (+0.1V\ vs\ SHE) \tag{7}$$

$$Positive\ Electrode: Mn^{2+} \rightleftharpoons Mn^{3+} + e^-\ (-1.51V\ vs\ SHE) \tag{8}$$

Unfortunately, Mn^{3+} is highly unstable and inclined to form manganese dioxide (MnO_2) *via* the following reaction-

$$2Mn^{3+} + 2H_2O \rightarrow Mn^{2+} + MnO_2$$
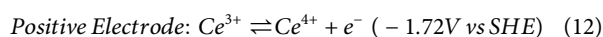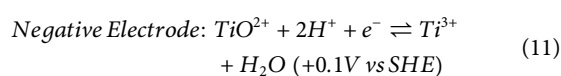$$+ 4H^+\ (Disproportionation\ Reaction) \tag{9}$$
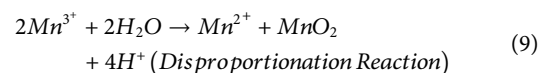
The precipitated MnO_2 particles start to aggregate and hinder the flow of electrolyte by blocking the pores of the membrane thereby reducing the columbic efficiency. So, it is required to reduce the formation of MnO_2 particles as well as to ensure that the MnO_2 particle are small enough to avoid aggregation and prevent membrane fouling (Kaku et al., 2016). Several approaches have been proposed for stabilization of Mn^{3+} such as by increasing the acidity, by increasing the Mn^{2+} concentration, or *via* complex formation (Davies, 1969). However, increasing Mn^{2+} concentration necessitates limiting the cycling of the cell to only 50% state of charge (SOC) to prevent Mn^{3+} disproportionation, thereby negating any advantages due to increased reactant concentration. On the other hand, the formation of Mn complexes (i.e., MnOOH) results in loss of electro-activity (Dong et al., 2015; Bahdad et al., 2021).

$$MnO_2 + H^+ + e^- \rightarrow MnOOH \tag{10}$$
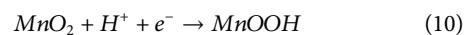
The disproportionation reaction and the morphology of MnO_2 were significantly influenced by addition of H_2SO_4 solution containing TiO^{2+} ions (Kaku et al., 2016). $TiOSO_4$ solutions of varying molarities was added to 1M $MnSO_4$ and the characteristic of the composite electrolyte was studied in the context of suppressing the disproportionation of Mn^{3+} ions. The MnO_2 aggregates were found to be > 1000 nm without adding $TiOSO_4$ or with the addition of 0.25M $TiOSO_4$ in $MnSO_4$. The particles size reduced to less than 100 nm with addition of 0.5M–1M of $TiOSO_4$ in $MnSO_4$ (Kaku et al., 2016). The optimal composition of 1.5 M $TiOSO_4$ in the 1 M $MnSO_4$ electrolyte improved the performance of the Ti-Mn RFB in terms of energy density to achieve ~11.75 Wh. L^{-1} (accounting for the electrolyte in both tanks) with coulombic efficiency of 99.8% and energy efficiency of 88.7%, both of which were stable over 40 cycles (Dong et al., 2015; Dong et al., 2017; Kaku et al., 2019). Unfortunately, the addition of $TiOSO_4$ with $MnSO_4$ also reduces the cell voltage by more than 100 mV and increases the cost of energy components (Kaku et al., 2016). An alternate approach using V^{5+} ions to stabilize the Mn electrolyte has also been proposed (Reynard et al., 2020). These V/Ti/Mn RFB systems will exhibit higher voltages compared to the Ti/Mn system given the lower standard electrode potential of the V^{3+}/V^{2+} couple (-0.26V vs SHE). But this system is economically unattractive given the increased cost associated with the use of vanadium and thus we do not believe this is a viable future direction. Various thicknesses of Nafion® i.e., Nafion® 115, Nafion® 212, Nafion® 211 have been

evaluated to investigate their impact on the performance of Ti-Mn RFBs. The energy efficiency was found to be function of separator thickness with the energy efficiency being 84%, 83%, and 81% for Nafion® 211 (25 μm), Nafion® 212 (51 μm), and Nafion® 115 (127 μm) respectively (Kaku et al., 2017).

Ti-Ce RFB: An alternative Ti based RFB which provides a higher OCP compared to, Ti-Fe and Ti-Mn RFBs, are Ti-Ce RFB. The OCP of Ti-Ce RFB is 1.61V, which results in higher operating power density at the same operating current density and higher energy density for the same electrolyte concentration compared to Ti-Fe and Ti-Mn systems (Sankarasubramanian et al., 2021). These RFBs can achieve a theoretical energy density of 19.4 Wh/L. The half-cell redox reactions of Ti-Ce RFB are represented by the following equations.

$$Negative\ Electrode: TiO^{2+} + 2H^+ + e^- \rightleftharpoons Ti^{3+} + H_2O\ (+0.1V\ vs\ SHE) \tag{11}$$

$$Positive\ Electrode: Ce^{3+} \rightleftharpoons Ce^{4+} + e^-\ (-1.72V\ vs\ SHE) \tag{12}$$

The Ce Pourbaix diagram shows that cerium ions are soluble in strong acids but forms stable, insoluble hydroxyl complexes above pH ~7. Given the exceptionally high standard reduction potential for Ce (the highest amongst all the catholyte candidates considered here), the stability of the supporting electrolyte is a particular concern - HCl and HNO$_3$ cannot be used due to their side reactions that produce Cl$_2$ and NO$_2$ respectively (Sankarasubramanian et al., 2021). The Ce^{4+}/Ce^{3+} redox couple exhibits unusual solubility behavior as a function of the supporting electrolyte (acid) concentration. The solubility of both species in this redox couple decreases in inverse proportion to H$_2$SO$_4$ concentration and the highest concentration achieved was 0.5M Ce in 1M H$_2$SO$_4$ (Xie et al., 2011b). But interestingly, in CH$_3$SO$_3$H, the solubility of Ce^{3+} decreases and the solubility of the Ce^{4+} increases with increasing acid concentration and this results in a solubility maximum of 0.9M Ce in 4M CH$_3$SO$_3$H (Kreh et al., 1989; Shi et al., 1989; Sankarasubramanian et al., 2021). Thus, the energy density of this system is circumscribed by the solubility of the Ce catholyte as TiOSO$_4$ is highly soluble in both H$_2$SO$_4$ and CH$_3$SO$_3$H (Sankarasubramanian et al., 2021). On the other hand, the Ti electrode is the rate-limit electrode (relevant for achieving higher operating current densities) as the rate constants of the Ce^{4+}/Ce^{3+} couple is 3x that of the Ti^{4+}/Ti^{3+} redox couple (Klingler and Kochi, 1981; Sankarasubramanian et al., 2021). Cyclic voltammetry shows the anodic to cathodic peak separation for Ti^{3+}/Ti^{4+} to be 1V and 0.67V for the Ce^{4+}/Ce^{3+} couple (Sankarasubramanian et al., 2021), indicating these reactions are not electrochemically reversible and suggesting high charge and discharge overpotentials (Bard and Faulkner, 2000). Nevertheless, in both H$_2$SO$_4$ and CH$_3$SO$_3$H supporting electrolytes, the Ti-Ce RFB exhibited nearly 100% coulombic efficiency with over 70% energy efficiency (charging and discharging at 100 mA/cm^2) during 1300 and 700 h of diurnal cycling, respectively (Sankarasubramanian et al., 2021). These cells employed highly permselective quaternary cardo-poly

ether ketone (QPEK-C) AEM separators (Yun et al., 2014; Yun et al., 2015; Yun et al., 2016) which demonstrated negligible crossover (<0.4%) over 1000 h of operation with 24 h cycle as compared to commercial CEM which suffers from drastic cation crossover and loss in capacity early in the cycling of the RFB (Sankarasubramanian et al., 2021).

3 Future Directions and Prospects

The Ti-X family of RFBs represent an interesting new direction in the development of aqueous RFB systems given their high theoretical energy density and economic competitiveness enabled by the high solubility and low cost of Ti. We anticipate the following future directions –

1) Unlocking the high energy density of the Ti electrolyte by pairing it with a stable and high solubility counter electrolyte. The long-term stability of the low pH Ti electrolytes needs to be demonstrated.
2) Catalyzing Ti^{4+}/Ti^{3+} redox kinetics to overcome its nature as the rate-limiting electrode. The catalysts should be low cost to preserve the cost advantage enjoyed by the Ti electrolyte.
3) Increasing the thermal stability of the Ti electrolyte to prevent TiO$_2$ formation by hydrolysis.
4) Using AEM and pore tailored PM instead of CEM to reduce crossover of the predominantly cationic redox active species, thereby enabling electrode decoupled RFBs. (Wang et al., 2018).

The continued development of these systems is anticipated to result in a commercially viable, high-energy density aqueous RFB that can economically be integrated into the electric grid.

Author contributions

SIUA and MS contributed equally to this manuscript. SIUA and MS prepared the first draft of the manuscript. All authors reviewed and revised the manuscript. SS conceived and supervised the project.

Funding

Conflict of interest

The authors declare that the research was conducted in the absence of any commercial or financial relationships that could be construed as a potential conflict of interest.

Publisher's note

All claims expressed in this article are solely those of the authors and do not necessarily represent those of their affiliated organizations, or those of the publisher, the editors and the reviewers. Any product that may be evaluated in this article, or claim that may be made by its manufacturer, is not guaranteed or endorsed by the publisher.

References

Archana, K. S., Suresh, S., Ragupathy, P., and Ulaganathan, M. (2020). Investigations on new Fe–Mn redox couple based aqueous redox flow battery. *Electrochimica Acta* 345, 136245. doi:10.1016/j.electacta.2020.136245

Bahdad, A. O. O. (2020). *Characterization of the electron transfer reaction mechanism of TiOSO4 and MnSO4 in sulfuric acid solution*. Kansas, US: University of Kansas.

Bahdad, A. O. O., Li, Y., and Van Nguyen, T. (2021). Characterization of the electrochemical behavior of $MnSO_4$ with and without $TiOSO_4$ in H_2SO_4 solution. *J. Electrochem. Soc.* 168 (7), 070524. doi:10.1149/1945-7111/ac0e4e

Bard, A. J. B., and Faulkner, L. R. (2000). *Electrochemical methods: Fundamentals and applications*. 2 ed. New York: Wiley.

Barry, E., Burns, R., Chen, W., De Hoe, G. X., De Oca, J. M. M., de Pablo, J. J., et al. (2021). Advanced materials for energy-water systems: The central role of water/solid interfaces in adsorption, reactivity, and transport. *Chem. Rev.* 121 (15), 9450–9501. doi:10.1021/acs.chemrev.1c00069

Beukenkamp, J., and Herrington, K. D. (1960). Ion-exchange investigation of the nature of titanium(IV) in sulfuric acid and perchloric acid. *J. Am. Chem. Soc.* 82 (12), 3025–3031. doi:10.1021/ja01497a014

Bhattarai, A., Whitehead, A. H., Schweiss, R., Scherer, G. G., Skyllas-Kazacos, M., Wai, N., et al. (2019). Anomalous behavior of anion exchange membrane during operation of a vanadium redox flow battery. *ACS Appl. Energy Mat.* 2 (3), 1712–1719. doi:10.1021/acsaem.8b01816

Chen, H., Cong, T. N., Yang, W., Tan, C., Li, Y., and Ding, Y. (2009). Progress in electrical energy storage system: A critical review. *Prog. Nat. Sci.* 19 (3), 291–312. doi:10.1016/j.pnsc.2008.07.014

Choe, Y-K., Tsuchida, E., Tokuda, K., Otsuka, J., Saito, Y., Masuno, A., et al. (2021). First-principles molecular dynamics simulation study on Ti4+ ion in aqueous sulfuric acid. *AIP Adv.* 11 (3), 035224. doi:10.1063/5.0038061

Comba, P., and Merbach, A. (1987). The titanyl question revisited. *Inorg. Chem.* 26 (8), 1315–1323. doi:10.1021/ic00255a024

Cservenyák, I., Kelsall, G. H., and Wang, W. (1996). Reduction of TiIV species in aqueous hydrochloric and sulfuric acids II. ECE model of the behaviour in sulfate media. *Electrochimica Acta* 41 (4), 573–582. doi:10.1016/0013-4686(95)00344-4

Cunha, Á., Martins, J., Rodrigues, N., and Brito, F. P. (2015). Vanadium redox flow batteries: A technology review. *Int. J. Energy Res.* 39 (7), 889–918. doi:10.1002/er.3260

Davies, G. (1969). Some aspects of the chemistry of manganese (III) in aqueous solution. *Coord. Chem. Rev.* 4 (2), 199–224. doi:10.1016/s0010-8545(00)80086-7

Dewage, H. H., Wu, B., Tsoi, A., Yufit, V., Offer, G., and Brandon, N. (2015). A novel regenerative hydrogen cerium fuel cell for energy storage applications. *J. Mat. Chem. A Mat.* 3 (18), 9446–9450. doi:10.1039/c5ta00571j

Dong, Y., Kaku, H., Miyawaki, H., Tatsumi, R., Moriuchi, K., and Shigematsu, T. (2017). Titanium-manganese electrolyte for redox flow battery. *SEI Tech. Rev.* 84, 35

Dong, Y-R., Shigematsu, T., Kumamoto, T., Kubata, M., and inventors (2012). *Sumitomo electric industries, ltd., assignee. Redox flow battery*. Alexandria, VA: United States Patent and Trademark Office.

Dong, Y. R., Kaku, H., Hanafusa, K., Moriuchi, K., and Shigematsu, T. (2015). A novel titanium/manganese redox flow battery. *ECS Trans.* 69 (18), 59–67. doi:10.1149/06918.0059ecst

Kaku, H., Yamaguchi, H., Dong, Y- R., Tatsumi, R., Miyatake, K., Moriuchi, K., et al. (2019). "A 10kW class Ti/Mn redox flow battery," in *ECS meeting abstracts* (IOP Publishing).

Fedkiw, P. S., and Watts, R. W. (1984). A mathematical model for the iron/chromium redox battery. *J. Electrochem. Soc.* 131 (4), 701–709. doi:10.1149/1.2115676

Funding opportunity announcement advanced research projects agency (2016). *Energy (arpa-E) duration addition to electricity storage (DAYS)*. Dep. Energy. Governmental Announcement.

Gong, K., Xu, F., Grunewald, J. B., Ma, X., Zhao, Y., Gu, S., et al. (2016). All-soluble all-iron aqueous redox-flow battery. *ACS Energy Lett.* 1 (1), 89–93. doi:10.1021/acsenergylett.6b00049

Gubler, L. (2019). Membranes and separators for redox flow batteries. *Curr. Opin. Electrochem.* 18, 31–36. doi:10.1016/j.coelec.2019.08.007

Holland-Cunz, M. V., Cording, F., Friedl, J., and Stimming, U. (2018). Redox flow batteries—concepts and chemistries for cost-effective energy storage. *Front. Energy* 12 (2), 198–224. doi:10.1007/s11708-018-0552-4

Jiang, H. R., Sun, J., Wei, L., Wu, M. C., Shyy, W., and Zhao, T. S. (2020). A high power density and long cycle life vanadium redox flow battery. *Energy Storage Mater.* 24, 529–540. doi:10.1016/j.ensm.2019.07.005

Jiang, T., Lin, H., Sun, Q., Zhao, G., and Shi, J. (2018). Recent progress of electrode materials for zinc bromide flow battery. *Int. J. Electrochem. Sci.* 13, 5603–5611. doi:10.20964/2018.06.34

Kaku, H., Dong, Y. R., Hanafusa, K., Moriuchi, K., and Shigematsu, T. (2016). Effect of Ti(IV) ion on Mn(III) stability in Ti/Mn electrolyte for redox flow battery. *ECS Trans.* 72 (10), 1–9. doi:10.1149/07210.0001ecst

Kaku, H., Kawagoe, Y., Dong, Y-R., Tatsumi, R., Moriuchi, K., and Shigematsu, T. (2017). Enhanced performance of Ti/Mn redox flow battery. *ECS Trans.* 77 (11), 173–183. doi:10.1149/07711.0173ecst

Kavan, L., O'Regan, B., Kay, A., and Grätzel, M. (1993). Preparation of TiO_2 (anatase) films on electrodes by anodic oxidative hydrolysis of $TiCl_3$. *J. Electroanal. Chem.* 346 (1), 291–307. doi:10.1016/0022-0728(93)85020-h

Klingler, R. J., and Kochi, J. K. (1981). Electron-transfer kinetics from cyclic voltammetry. Quantitative description of electrochemical reversibility. *J. Phys. Chem.* 85 (12), 1731–1741. doi:10.1021/j150612a028

Kotsyubynsky, V. O., Myronyuk, I. F., Chelyadyn, V. L., Hrubiak, A. B., Moklyak, V. V., and Fedorchenko, S. V. (2017). The effect of sulphate anions on the ultrafine titania nucleation. *Nanoscale Res. Lett.* 12 (1), 369. doi:10.1186/s11671-017-2144-3

Kreh, R. P., Spotnitz, R. M., and Lundquist, J. T. (1989). Mediated electrochemical synthesis of aromatic aldehydes, ketones, and quinones using ceric methanesulfonate. *J. Org. Chem.* 54 (7), 1526–1531. doi:10.1021/jo00268a010

Leung, P. K., Ponce-de-León, C., Low, C. T. J., Shah, A. A., and Walsh, F. C. (2011). Characterization of a zinc–cerium flow battery. *J. Power Sources* 196 (11), 5174–5185. doi:10.1016/j.jpowsour.2011.01.095

Lingane, J. J., and Kennedy, J. H. (1956). Polarography of titanium in strong mineral acid media. *Anal. Chim. Acta* 15, 294–300. doi:10.1016/0003-2670(56)80053-6

Lokhande, C., Sun-Ki, M., Jung, K-D., and Joo, O-S. (2004). Cathodic electrodeposition of amorphous titanium oxide films from an alkaline solution bath. *J. Mater. Sci.* 39 (21), 6607–6610. doi:10.1023/b:jmsc.0000044903.93296.a4

Lokhande, C. D., Min, S-K., Jung, K-D., and Joo, O-S. (2005). Cathodic electrodeposition of amorphous titanium oxide films from an alkaline solution bath. *J. Mat. Sci.* 40 (2), 491–494. doi:10.1007/s10853-005-6111-5

Lu, W., Yuan, Z., Zhao, Y., Zhang, H., Zhang, H., and Li, X. (2017). Porous membranes in secondary battery technologies. *Chem. Soc. Rev.* 46 (8), 2199–2236. doi:10.1039/c6cs00823b

Mangold, L., Halleux, H., Leclerc, S., Moncomble, A., Cote, G., and Chagnes, A. (2021). New insights for titanium(iv) speciation in acidic media based on UV-visible and 31P NMR spectroscopies and molecular modeling. *RSC Adv.* 11 (43), 27059–27073. doi:10.1039/d1ra04284j

Miyanaga, T., Watanabe, I., and Ikeda, S. (1990). Structures of hydrated titanium and vanadium ions in aqueous solutions studied by X-ray absorption spectroscopy. *Bull. Chem. Soc. Jpn.* 63 (11), 3282–3287. doi:10.1246/bcsj.63.3282

Molina, P. I., Kozma, K., Santala, M., Falaise, C., and Nyman, M. (2017). Aqueous bismuth titanium–oxo sulfate cluster speciation and crystallization. *Angew. Chem. Int. Ed.* 56 (51), 16277–16281. doi:10.1002/anie.201709539

Morris, D. F., MacCarthy, J. D., and Newton, R. J. (1978). Outer-sphere and inner-sphere interactions in the formation of metal-ion nitrate complexes. *Electrochimica Acta* 23 (12), 1383–1386. doi:10.1016/0013-4686(78)80021-8

Naresh, Rp, Mariyappan, K., Dixon, D., Ulaganathan, M., and Ragupathy, P. (2021). Investigations on new electrolyte composition and modified membrane for high voltage Zinc–Manganese hybrid redox flow batteries. *Batter. Supercaps* 4 (9), 1464–1472. doi:10.1002/batt.202100071

Oldenburg, F. J., Bon, M., Perego, D., Polino, D., Laino, T., Gubler, L., et al. (2018). Revealing the role of phosphoric acid in all-vanadium redox flow batteries with DFT calculations and *in situ* analysis. *Phys. Chem. Chem. Phys.* 20 (36), 23664–23673. doi:10.1039/c8cp04517h

Pourbaix, M. (1966). *Atlas of electrochemical equilibria in aqueous solutions*. Oxford; New York: Pergamon Press.

Prifti, H., Parasuraman, A., Winardi, S., Lim, T. M., and Skyllas-Kazacos, M. J. M. (2012). Membranes for redox flow battery applications. *Membranes* 2 (2), 275–306. doi:10.3390/membranes2020275

Qiao, L., Fang, M., Liu, S., Zhang, H., and Ma, X. (2022). New-generation iron–titanium flow batteries with low cost and ultrahigh stability for stationary energy storage. *Chem. Eng. J.* 434, 134588. doi:10.1016/j.cej.2022.134588

Raja, M., Khan, H., Sankarasubramanian, S., Sonawat, D., Ramani, V., and Ramanujam, K. (2021). Binder-free thin graphite fiber mat sandwich electrode architectures for energy-efficient vanadium redox flow batteries. *Catal. Today* 370, 181–188. doi:10.1016/j.cattod.2021.02.012

Reynard, D., Maye, S., Peljo, P., Chanda, V., Girault, H. H., and Gentil, S. (2020). Vanadium–manganese redox flow battery: Study of MnIII disproportionation in the presence of other metallic ions. *Chem. Eur. J.* 26 (32), 7250–7257. doi:10.1002/chem.202000340

Sankarasubramanian, S., Zhang, Y., He, C., Gregory, T., and Ramani, V. (2021). *An aqueous, electrode-decoupled redox-flow battery for long duration energy storage*. Research. Square. Pre-print.

Sankarasubramanian, S., Zhang, Y., and Ramani, V. (2019). Methanesulfonic acid-based electrode-decoupled vanadium–cerium redox flow battery exhibits significantly improved capacity and cycle life. *Sustain. Energy Fuels* 3 (9), 2417–2425. doi:10.1039/c9se00286c

Savinell, R. F., Liu, C. C., Galasco, R. T., Chiang, S. H., and Coetzee, J. F. (1979). Discharge characteristics of a soluble iron-titanium battery system. *J. Electrochem. Soc.* 126 (3), 357–360. doi:10.1149/1.2129043

Selverston, S., Savinell, R. F., and Wainright, J. S. (2017). Zinc-iron flow batteries with common electrolyte. *J. Electrochem. Soc.* 164 (6), A1069–A1075. doi:10.1149/2.0591706jes

Shepherd, S. (2013). *An investigation into aqueous titanium speciation utilising electrochemical methods for the purpose of implementation into the sulfate process for titanium dioxide manufacture*. Callaghan, NSW: University of Newcastle. Degree Thesis.

Shi, L., Wang, W., Wang, Y., and Huang, Y. (1989). The first example of a catalytic Wittig-type reaction. Tri-n-butylarsine-catalyzed olefination in the presence of triphenyl phosphite. *J. Org. Chem.* 54 (9), 2027–2028. doi:10.1021/jo00270a001

Skyllas-Kazacos, M., Chakrabarti, M. H., Hajimolana, S. A., Mjalli, F. S., and Saleem, M. (2011). Progress in flow battery research and development. *J. Electrochem. Soc.* 158 (8), R55. doi:10.1149/1.3599565

Sole, K. C. (1999). Recovery of titanium from the leach liquors of titaniferous magnetites by solvent extraction: Part 1. Review of the literature and aqueous thermodynamics. *Hydrometallurgy* 51 (2), 239–253. doi:10.1016/s0304-386x(98)00081-4

Thaller, L. H., and inventor (1976). The United States of America as represented by the Administrator of the National Aeronautics and Space Administration, assignee." in *Electrically rechargeable redox flow cell*. The United States of America patent US3996064A.

Tsurumura, T., Ohkubo, K., Tanaka, T., and Fujii, K. (2020). Structural study on Ti-ion complexes in concentrated aqueous electrolytes: Raman spectroscopy and high-energy X-ray total scattering. *J. Mol. Liq.* 305, 112867. doi:10.1016/j.molliq.2020.112867

Tsurumura, T., Tanaka, T., Yagi, K., Morita, M., Kameda, Y., and Fujii, K. (2018). Local structures of titanium-ion complexes in redox flow battery electrolytes as revealed by X-ray scattering with difference analysis. *J. Mol. Liq.* 261, 468–472. doi:10.1016/j.molliq.2018.04.074

Ulaganathan, M., Suresh, S., Mariyappan, K., Periasamy, P., and Pitchai, R. (2019). New zinc–vanadium (Zn–V) hybrid redox flow battery: High-voltage and energy-efficient advanced energy storage system. *ACS Sustain. Chem. Eng.* 7 (6), 6053–6060. doi:10.1021/acssuschemeng.8b06194

Varcoe, J. R., Atanassov, P., Dekel, D. R., Herring, A. M., Hickner, M. A., Kohl, P. A., et al. (2014). Anion-exchange membranes in electrochemical energy systems. *Energy Environ. Sci.* 7 (10), 3135–3191. doi:10.1039/c4ee01303d

Wang, Y., Lin, M., and Wan, C. (1984). A study of the discharge performance of the Ti/Fe redox flow system. *J. power sources* 13 (1), 65–74. doi:10.1016/0378-7753(84)80054-3

Wang, Z., Sankarasubramanian, S., and Ramani, V. (2018). Advances in anion exchange membranes for electrochemical energy conversion. *Curr. Opin. Electrochem.* 12, 240–245. doi:10.1016/j.coelec.2018.11.011

Wang, Z., Sankarasubramanian, S., Willey, J., Feng, H., Xu, H., and Ramani, V. (2021). Engineering block co-polymer anion exchange membrane domains for highly efficient electrode-decoupled redox flow batteries. *Sustain. Energy Fuels* 5 (14), 3606–3616. doi:10.1039/d1se00543j

Wu, C. D., Calvo, E. J., and Yeager, E. (1983). *Electrochemical studies of redox systems for energy storage*. Cleveland, OH: Center for Electrochemical Sciences. NASA.

Xie, Z., Xiong, F., and Zhou, D. (2011). Study of the Ce3+/Ce4+ redox couple in mixed-acid media (CH3SO3H and H2SO4) for redox flow battery application. *Energy fuels.* 25 (5), 2399–2404. doi:10.1021/ef200354b

Xie, Z., Zhou, D., Xiong, F., Zhang, S., and Huang, K. (2011). Cerium-zinc redox flow battery: Positive half-cell electrolyte studies. *J. Rare Earths* 29 (6), 567–573. doi:10.1016/s1002-0721(10)60499-1

Yun, S., Parrondo, J., and Ramani, V. (2015). A vanadium-cerium redox flow battery with an anion-exchange membrane separator. *ChemPlusChem* 80 (2), 412–421. doi:10.1002/cplu.201402096

Yun, S., Parrondo, J., and Ramani, V. (2016). Composite anion exchange membranes based on quaternized cardo-poly(etherketone) and quaternized inorganic fillers for vanadium redox flow battery applications. *Int. J. Hydrogen Energy* 41 (25), 10766–10775. doi:10.1016/j.ijhydene.2016.04.060

Yun, S., Parrondo, J., and Ramani, V. (2014). Derivatized cardo-polyetherketone anion exchange membranes for all-vanadium redox flow batteries. *J. Mat. Chem. A* 2 (18), 6605–6615. doi:10.1039/c4ta00166d

Zhao, H., Wu, Q., Hu, S., Xu, H., and Rasmussen, C. N. (2015). Review of energy storage system for wind power integration support. *Appl. Energy* 137, 545–553. doi:10.1016/j.apenergy.2014.04.103

Zhen, Y., Zhang, C., Yuan, J., Zhao, Y., and Li, Y. (2020). A high-performance all-iron non-aqueous redox flow battery. *J. Power Sources* 445, 227331. doi:10.1016/j.jpowsour.2019.227331